Int. J. Electrochem. Sci., 14 **(2019)** 6315 – 6324, doi: 10.20964/2019.07.73

International Journal of ELECTROCHEMICAL SCIENCE
www.electrochemsci.org

Short Communication

First-principle Study on Sr-doped $LiNi_{0.5}Mn_{1.5}O_4$

Xinghua Liang[1,2], Yunting Wang[1],Di Han[1], Jie Mao[2], Lingxiao Lan[1]*

[1] Guangxi Key Laboratory of Automobile Components and Vehicle Technology, Guangxi University of Science & technology, Liuzhou 545000, China;
[2]Guangdong Institute of New Materials,National Engineering Laboratory for Modern Materials Surface,Guangdong Academy of Science,Guangzhou 510651,China
[*]E-mail: 904204647@qq.com

Received: 15 March 2019 / *Accepted:* 15 May 2019 / *Published:* 10 June 2019

Applying supersoft pseudopotential plane wave method of the first principle based on functional theory to investigate the band and density of states of $LiNi_{0.5}Mn_{1.5}O_4$ and Sr^{2+} doped $LiNi_{0.5}Mn_{1.5}O_4$.Theoretical caculations demonstrated that $LiNi_{0.5}Mn_{1.5}O_4$ is a conductor material as well as the site of Mn doping Sr^{2+} will increase the bands number of $LiNi_{0.5}Mn_{1.5}O_4$.Furthermore,after $LiNi_{0.5}Mn_{1.5}O_4$ doping Sr^{2+},it will help to shorthen bond length between Mn-O and Ni-O bond, making the crystal structure more stable.The distance of Li-O bond is elongated,which will benefit the diffustion in the 3D channel thereby increasing the electronic conductivity and the rate performance of $LiNi_{0.5}Mn_{1.5}O_4$.According to electronic density analysis,the hybridization of Mn 3d and O 2p states is more obvious,which indicating that the covalent bond formed by the two atoms is stronger and the crystal structure is not easily collapsed, thereby improving the cycle stability of the material.

Keywords: $LiNi_{0.5}Mn_{1.5}O_4$;lithium-ion batteries;first-principles

1. INTRODUCTION

Rechargeble lithium-ion batteries have been considered as the most promising and attractive new power sources[1-3].Recently,it is widely utilized in various fields such as electric devices including digital cameras and mobile phones,electric vehicles and energy storage systems may be attributed to their long cycle life and high energy density.Cathodes materials play an important role in lithium-ion batteries,which will directly affect the performance of batteries[4-6].Spinel $LiNi_{0.5}Mn_{1.5}O_4$ material is one of the potential candidates cathode materials for secondary lithium-ion battery not only due to its price moderate and non-toxicity compared to the present applicationt of $LiCoO_2$ but also it possess a good deal of advantages such as high energy density,environment friendly,high voltage and so on[7].Spinel $LiNi_{0.5}Mn_{1.5}O_4$ material has been studied extensively becuase of it shows significant value and bright application prospect in the fields of hight performance battery.Ohzuku [8] investigated

the redox potentials for $LiM_{0.5}Mn_{1.5}O_4$ (M: 3d-transition metal).It is found that the chromium, iron, cobalt, nickel, or copper containing sample exhibited common solid-state redoxpotentials at 5.0±0.2 V in addition to 4.0±0.1 V vs. Li^+/Li. Aurbach[9] studied the electrochemical properties of $LiNi_{0.5}Mn_{1.5}O_4$ at 60°C,and the voltammograms indicated that the resolution of the sets of anodic and cathodic peaks at 60°C is better, it means that the $LiNi_{0.5}Mn_{1.5}O_4$ electrodes should conduct faster kinetics.

However, Spinel $LiNi_{0.5}Mn_{1.5}O_4$ material still suffers from the serious capacity attenuation,which is surely ascribable to corrosion reaction between the cathode surface and the electrolyte and is the primary obstacle to its applications in practice.To address these issues, a number of research groups have investigated the effects of coating oxide and doping on the cathode materials Spinel $LiNi_{0.5}Mn_{1.5}O_4$,which are effective ways to enhance its performance.For instance,Jaesang Yoon[10]investigated the effects of $LiNi_{0.5}Mn_{1.5}O_4$ doped Zr on its structural behavior,The results show that Zr doping has great potential for high performance applications. If the material is optimized, it is expected to provide structural stability during repeated cycles.In addition,MaoHuang Liu[11] studied the $LiNi_{0.5}Mn_{1.5}O_4$ gradient-doped with Mg by the methods of co-precipitation,which indicates Mg doping $LiNi_{0.5}Mn_{1.5}O_4$ cathode material has an excellent electrochemical performance due to it can effectively reduce the side-reaction between the cathode and the electrolyte as will as restrain the formation of the SEI layer during the electrochemical cycle. In addition, 4d-transition metal ions such as Rh, Ru etc. were also adopted as dopants to significantly enhance the electrochemical performance of the Ni-Mn spinels.[12-16] Doping different elements into the crystal of $LiNi_{0.5}Mn_{1.5}O_4$ can alter and enhance its properties to achieve better performance.To some extent,the density of states and the band structure of the material will determine the physical and chemical properties of the material.Therefore, accurate simulation calculations of the crystal structure of the material can identify potential doping mechanisms,which can guide experiments and design high performance cathode materials.

The above review of the previous studies shows that it is necessary to study the structural of spinel $LiNi_{0.5}Mn_{1.5}O_4$ theoretically.In the present work,we carry out first-principles calculations on the crystal and electronic structures of pure $LiNi_{0.5}Mn_{1.5}O_4$ and after doping Sr^{2+} on $LiNi_{0.5}Mn_{1.5}O_4$. The parameters including band structure,density of states,as well as its bonds population analysis.

2. CALCULATION METHOD

The analysis of the electronic structure of materials is based on the density functional theory of Kohn-Sham theorem [17].In this investigation,the first-principle calculations of the electronic structure of materials were implemented in CASTEP code of Material Studio 6.0[18].The optimization of crystal structure is carryed out by the framework of DFT (density functional theory)[19].In addition,plane-wave pseudopotentia [20-22] are often utilized to investigate the behavior of interaction between ions and electrons because of their advantages in efficiency and reliability.For the purpose of further enhance the accuracy of calculation,a gradient approximation method of electron density, such as generalized gradient approximation (GGA), which is introduced in the exchange correlation function to deal with the problem of electron density non-uniformity.The Perdew-Burke-Ernzerhof (PBE)

method is utilized to describe the exchange-related potentials to acquire the charge density and total energy of the electronic structure of the material[23-25]. A Hubbard-type correction U was considered thanks to the extremely correlated property of the transition metal 3d electrons[26,27].Here,the (Ni,Mn) site U value was set to 6.0 and 5.0 eV, respectively [28].

The Kohn-Sham wave functions of valence electrons are expanded by a plane-wave basis.In this work,the convergence tests of k-points and energy cut-off were carefully carried out before optimization of the crystal structure calculations.After the convergence analysis we choose the energy cut-off of the plane-wave basis was 500 eV, which was enough to the total energy and geometry of $LiNi_{0.5}Mn_{1.5}O_4$ structure.Applying a 5×5×5 Monkhorst pack K-point mesh[29]for structural of the $LiNi_{0.5}Mn_{1.5}O_4$ optimizations, which are relaxed till the force on each atom is less than 0.03 eV/Å and an energy convergence criteria is 1.0×10^{-5} eV/Å for the gradient.The states of Li($1s^2 2s^1$), Mn($3s^2 3p^6 3d^5 4s^2$),Ni($3s^2 3p^6 3d^8 4s^2$),O($2s^2 2p^4$)and Sr($4s^2 4p^6 5s^2$)are treated as valence states.

3. RESULTS AND DISCUSSION

3.1 Structure characterization

$LiNi_{0.5}Mn_{1.5}O_4$ has cubic spinel structure and it posses two crystal structure,one depending type is the Ni/Mn ordered $P4_332$ phase and the other one is Ni/Mn disordered Fd-3m phase[30].It mainly depend on the temperature and atomosphere ,as well as the other conditions in the heat treatment process.The structural results demonstrate that employing the ordered crystal structure of materials to build mode will be more effective due to the disordered structure distribution feature complexity will bring difficulties in the calculation of the first principle.In the ordered spinel structure,the transition metal ions nickel and manganese occupy 4b and 12d position,respectively. The oxygen atoms occupy the 8c and 24e position, and the lithium ions occupy the 8c position. Octahedral vacancy 16c is split into ordered 4a and 12d positions,a ratio of 1:3.Lithium ions diffuses along two paths,which the one diffusion path of lithium ions is 8c to 4a and the other one is 8c to 12d.The calculated and experimental lattice parameters are listed in Table 1, where the results available from other works are also given for comparison. It is found that our calculated results are reasonably in agreement with other reports and experimental values.The ordered structure applied to calculate is shown in Fig.1(a) and (b).

After the crystal cell is established in the software and its geometric structure is optimized.The lattice constants of $LiNi_{0.5}Mn_{1.5}O_4$ before and after optimization are shown in the following table 1 and the model establishment is reliable due to the error between the optimized value and the experimental value is small.Then,the structure of the cell was optimized again by replacing one manganese atom with one indium atom.The lattice constants,volume and Fermi energy levels before and after structural optimization are also shown in the following table1.As we can see clearly,the volume of $LiNi_{0.5}Mn_{1.5}O_4$ doped with indium atoms is smaller than it used to be.It is demonstrated that the doped crystal structure is more stable and also means that the improvement of material's cycle performance,which is in agreement with reports of TingFengYi *et al.*[31],demonstrating the substitutions of Cr^{3+} simultaneously for both Mn^{4+} and Ni^{2+} will suppress the 4V plateau and increase

the 5V capacity and has an excellent capacity retention ,as well as better coulombic efficiency.

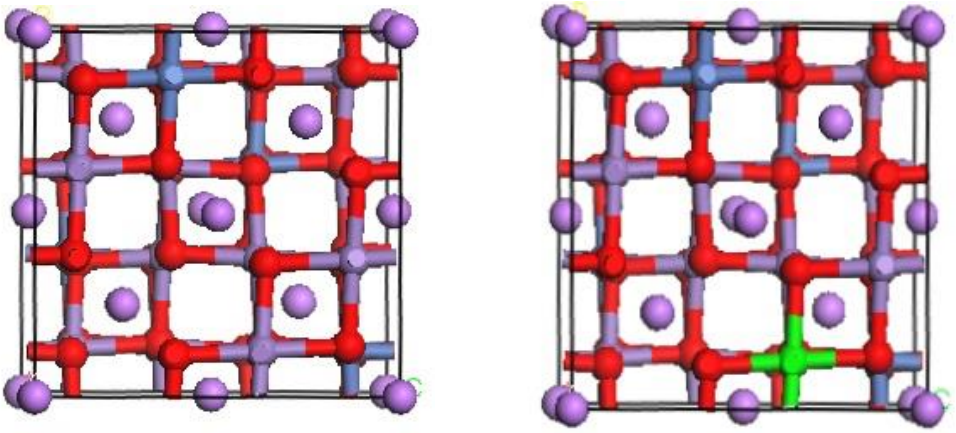

(a) (b)

Figure 1. Cell model of the (a) $LiNi_{0.5}Mn_{1.5}O_4$ and (b) $LiNi_{0.5}Mn_{1.375}Sr_{0.125}O_4$.

Table 1. Lattice parameter and volume of $LiNi_{0.5}Mn_{1.5}O_4$ and $LiNi_{0.5}Mn_{1.375}Sr_{0.125}O_4$

Sample	Lattice parameter （a/Å）	Angle（°）	Volume （a/Å）
$LiNi_{0.5}Mn_{1.5}O_{4(Experimental)}$[32]	a=b=c=8.174	α =90	546.187
$LiNi_{0.5}Mn_{1.5}O_{4(Initial\ value)}$	a=b=c=8.245	α=90°	560.495
$LiNi_{0.5}Mn_{1.5}O_{4(Optimized)}$	a=b=c=8.143	α=90°	540.659
$LiNi_{0.5}Mn_{1.375}Sr_{0.125}O_{4(Optimized)}$	a=b=8.282 c=8.283	α=92.567° γ=87.588°	566.486

3.2. Band structure

To further understand the microstructure of pure phase $LiNi_{0.5}Mn_{1.5}O_4$ and Sr^{2+} doped $LiNi_{0.5}Mn_{1.5}O_4$,the band structure and density of states (DOS) of them were also calculated by using GGA method.The energy band structure of the high-symmetry direction of the first Brillouin zone pure phase $LiNi_{0.5}Mn_{1.5}O_4$ and after the Sr^{2+} doped $LiNi_{0.5}Mn_{1.5}O_4$ is calculated.The final calculation results are shown in the figure2(a) and (b),respectively.As we can see it clearly that the number of energy bands of Sr^{2+} doped $LiNi_{0.5}Mn_{1.5}O_4$ is more than pure $LiNi_{0.5}Mn_{1.5}O_4$ .It is worth noting that the value are small than the experiment result,which mainly caused by the calculation value of generalized gradient approximation(GGA) which widespread the calculated value error.But the overall trend change of energy structure is consistent with the experimental value so that the energy gap based on density functional calculation is reliability.By compare figure (a) with figure (b),It can be found that the number of Sr^{2+} doped $LiNi_{0.5}Mn_{1.5}O_4$ bands increases and the forbidden band width narrows.This phenomenon demonstrated that the narrow band gap is beneficial for electron transition and thus increases the electrical conductivity of the material.

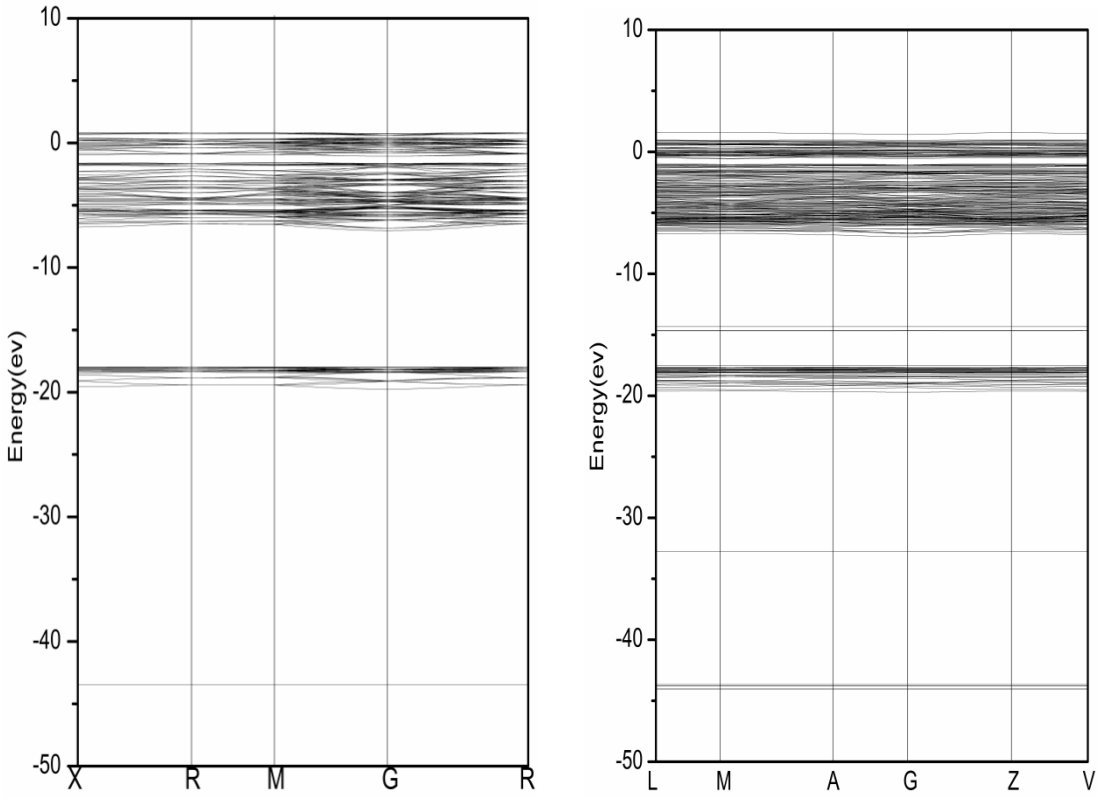

(a) (b)

Figure 2. Energy bandstructures of the (a) $LiNi_{0.5}Mn_{1.5}O_4$ and (b) $LiNi_{0.5}Mn_{1.375}Sr_{0.125}O_4$

3.3. Density of state

The calculation of electron density of states (DOS) and projected electron density of states (PDOS) were shown in Fig. 3.From Fig. 3,they have almost the same total density of states,which means the crystal structure did not change obviously after doping.It was also indicated that the energy band of Sr^{2+} doped $LiNi_{0.5}Mn_{1.5}O_4$ system is mainly distributed between -44.5 and 0.12eV.The density of states is mainly determined by the interation of Mn,Ni,O and Sr. It is also noteworthy that valence bands near the Fermi level were mainly attributed to Mn 3d, and O 2p states hybridized and/or mixed with small amount of Ni 3d states,while the energe span of Li is between -44.5 and -42.7eV.The peak shape of Li is sharper, indicating a smaller contribution to the total density of states.In other words,the sharp peak shape of lithium ions indicates that the localization of electrons is severe,which makes it easier for lithium ions to be inserted or removed in the crystal lattice of Sr^{2+} doped $LiNi_{0.5}Mn_{1.5}O_4$. The conduction bands between -20 eV and -14 eV were dominated by the O 2p states with some hybridization with Sr 2p states.Furthermore,it is worth addressing that the replacements of Mn atoms by Sr atoms also make the energy band of O 2p states increased evidently,presenting a correlation between O 2p and Mn 3d states more strengthen by the induction of Sr ions.It also reveals strong hybridization between Mn-3d and O-2p states,which covalent bond of them are hard to destroy.On the whole,the crystal structure of Sr^{2+} doped $LiNi_{0.5}Mn_{1.5}O_4$ become more stable,which is beneficial to improve the cycling perfomance of the material.The result agrees with Jing Mao[33] ,where Co doping is found to improve the cycling stability and and rate capability of the Ni-Mn spine.

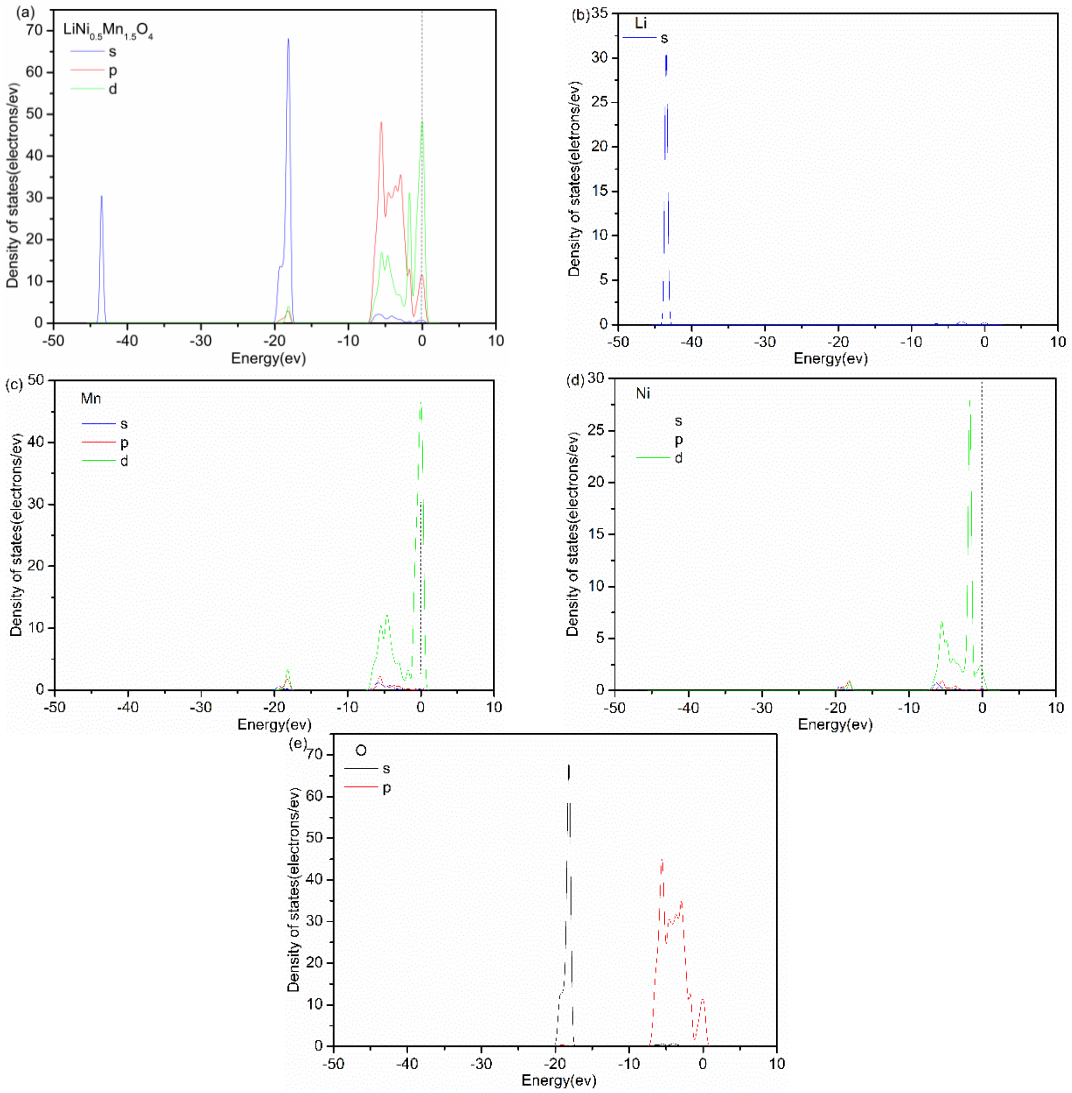

Figure 3. Density map of $LiNi_{0.5}Mn_{1.5}O_4$(a) and distribution of Li(b),Mn(c),Ni(d),O(e) element

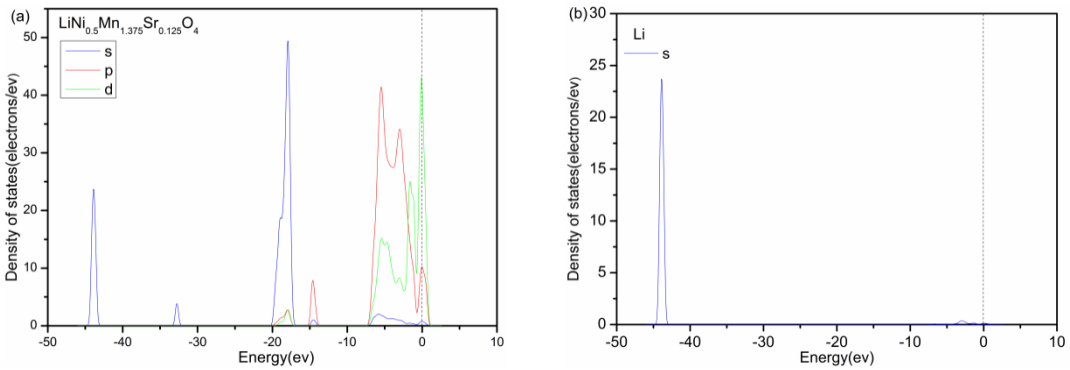

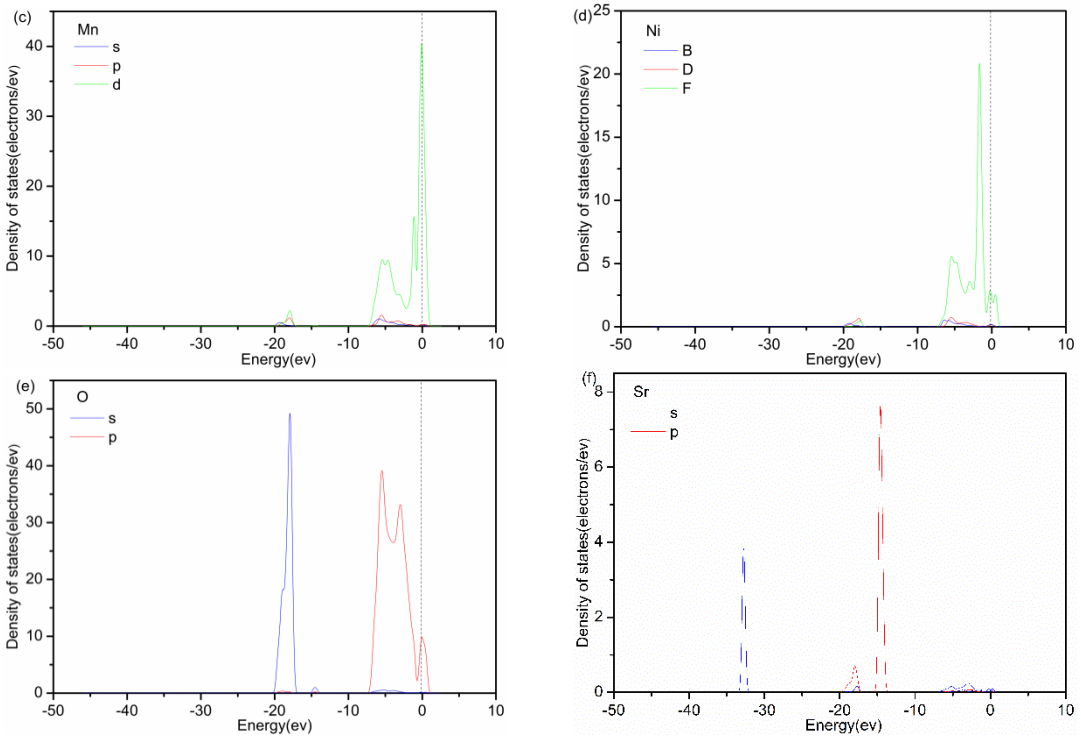

Figure 4. Density map of $LiNi_{0.5}Mn_{1.375}Sr_{0.125}O_4$ (a) and distribution of Li(b),Mn(c),Ni(d),O(e) and Sr(f) element

3.4. Population analysis

The height hybridization also demonstrates strong covalent interaction between Mn and O ions.In order to further disccution,the population analysis of pure phase $LiNi_{0.5}Mn_{1.5}O_4$ and Sr^{2+} doped $LiNi_{0.5}Mn_{1.5}O_4$ is performed and the results are shown in Table 2,3,4 and 5. The population number can be understood as the arrangement of electrons outside the nucleus. In this module ,the s,p,d and total electron numbers and the number of charges of each atom in the unit cell are calculated.From Table 2 and 3,it is clear the Li ions calculated value of the charge is +1.04e and +1.01e,respectively,which is close to the theoretical value of +1e.This kind of phenomenon reveals that the Li ions exhibits strong ionic bond characteristice,it will ensure the Li ions to move more freely without destroying the layer sructure of the anode material,so as to improve the material recycling performance.However, O and Mn exhibit strong covalent bond characteristics, such as oxygen 2P electrons,only 4.74,not 6.Figure 3 after doping is compared with Figure 2, the charge number of lithium ion is small and remains near 1.The ion is always +1 means it does not participate in electron sharing and exhibits strong ion characteristics.The 2p eletronic of O appeared to differentiate, which may be due to the induction of the d orbital of Sr.

Table 2. Atomic orbital distribution of $LiNi_{0.5}Mn_{1.5}O_4$

	s	p	d	Total	Charge(e)
Li	1.96	0	0	1.96	1.04
O	1.88	4.74	0	6.62	-0.62
Mn	0.3	0.4	5.58	6.28	0.72
Ni	0.42	0.57	8.33	9.32	0.68

Table 3. Atomic orbital distribution of $LiNi_{0.5}Mn_{1.375}Sr_{0.125}O_4$

	s	p	d	Total	Charge(e)
Li	1.99	0	0	1.99	1.01
O	1.88	4.81	0	6.68	-0.68
Mn	0.3	0.42	5.56	6.29	0.71
Ni	0.42	0.61	8.33	9.35	0.65
Sr	2.17	5.99	0.84	9	1

It can be seen from the comparison between Table 3(a) and (b),the overlapping population value of Mn-O bond and Ni-O bond increased significantly from 0.29 to 0.42 ,0.32 to 0.36,respectively.These observations consistent with the previous LSDA calculations that are performed by Koyama *et al*.[34]This phenomenon indicates that the larger positive value of the overlapping population, the stronger the covalent bond formed between the two atoms, and the combination of them is also more stable.Table 3(a) and (b) also can found that the length of Li-O bond is increased from 1.89 to 1.92.

Table 4. The overlap population and bond length change of $LiNi_{0.5}Mn_{1.5}O_4$

Bond	Population	Length(a)
Li-O	-0.02	1.89190
Mn-O	0.29	1.93679
Ni-O	0.32	1.95069

Table 5. The overlap population and bond length change of $LiNi_{0.5}Mn_{1.375}Sr_{0.125}O_4$

Bond	Population	Length(a)
Li-O	-0.02	1.92459
Mn-O	0.42	1.87263
Ni-O	0.36	1.90684
Sr-O	0.13	2.35567

The significant increase in bond length means that Li ions are more easily separated from the bond and are freed in the crystal lattice.In addition,the length of Mn-O bond and Ni-O bond slightly reduced,this will mean that when the lithium ion is deintercalated in the crystal structure, the crystal

structure will be more stable and not easy to collapse.In general,the crystal structure of the Sr^{2+} doped $LiNi_{0.5}Mn_{1.5}O_4$ is more stable, thereby improving the cycle performance of the material.

4.CONCLUSIONS

First-principles calculations in the GGA have been employed to investigate the pure phase $LiNi_{0.5}Mn_{1.5}O_4$ and the effection of Sr^{2+} doped $LiNi_{0.5}Mn_{1.5}O_4$.It is found that Li atoms will be easier diffuse into the doping $Sr^{2+}$of $LiNi_{0.5}Mn_{1.5}O_4$ lattice due to the Li-O bond is increased from 1.89 to 1.92 and the strong covalency of Mn-O and Ni-O bond,it also means the improvement of material cycle stability and makes doping Sr^{2+} of $LiNi_{0.5}Mn_{1.5}O_4$ to be a potential application in the positive electrode material of the battery.We believe that the exploration of this research will provide a powerful reference for the application of cathode materials for next-generation high-power lithium-ion batteries.

ACKNOWLEDGEMENTS
This work was supported by Fund Project of Guangxi Key Laboratory of Automobile Components and Vehicle Technology, Guangxi University of Science and Technology (No.2017GKLACVTZZ04); Innovation Project of GuangXi University of Science and Technology Graduate Education(YCSW2018202,YCSW2019210);GDAS' Special Project of Science and Technology Development（N0.2017GDAS CX-0202）; Innovation Team Project of GuangXi University of Science and Technology(No.3).

References

1. X. H. Liang, Y. C. Zhao, D. Han, J. Mao, L. X. Lan, Int. *J. Electrochem. Sci.*, 14 (2019) 717.
2. C. Sun, J. Liu, Y. Gong, D. P. Wilkinson, J. Zhang, *Nano Energy*, 33 (2017) 363.
3. S. J. Gerssen-Gondelach, A. P. C. Faaij, *J. Power Sources*, 212 (2012) 111.
4. X. H. Liang, S. Lin, Y. S. Liu, T. J. Liu, C. C. Ye, S. B. Zeng, *Adv. Mater. Res*., 860 (2014) 956.
5. A. Kraytsberg, Y. Ein-Eli, *Adv. Energy Mater.*, 2 (2012) 922.
6. M. Hu, X.L.Pang, Z.Zhou, *J. Power Sources*, 237 (2013) 229.
7. P. Manikandan, P. Periasamy, R. Jagannathan, *J. Power Sources*, 264 (2014) 299.
8. T. Ohzuku, S. Takeda, M. Iwanaga, *J. Power Sources*, 81 (1999) 90.
9. D. Kovacheva, B.Markovsky, G. Salitra, Y. Talyosef, M. Gorova, E. Levi, M. Riboch, H-J. Kim, D. Aurbach, *Electrochim. Acta*, 50 (2005) 5553.
10. J. Yoon, M. Jeong, I. T. Bae, K. W. Nam, W. S. Yoon, *J. Power Sources*, 368 (2017) 1.
11. M. H. Liu, H. T. Huang, C. M. Lin, J. M. Chen, S. C. Liao, *Electrochim. Acta*, 120 (2014) 133.
12. N. Kiziltas-Yavuz, A. Bhaskar, D. Dixon, M. Yavuz, K. Nikolowski, L. Lu, R. A. Eichel, H. Ehrenberg, *J. Power Sources*, 267 (2014) 533.
13. P. Wu, X. L. Zeng, C. Zhou, C. F. Gu, D. G. Tong, *Mater. Chem. Phys*., 138 (2013) 716.
14. R. Singhal, M. S. Tomar, S. R. Das, J. G. Burgos, S. P. Singh, A. Kumar, R. S. Katiyar, *Electrochem. Solid State Lett*., 10 (2017) A163.
15. H. Wang, H. Xia, M. O. Lai, L. Liu, *Electrochem. commun*, 11 (2009) 1539.
16. H. Wang, T. A. Tan, P. Yang, M. O. Lai, L. J. Lu, *Phys. chem*, 115 (2011) 6102.
17. H. J. Song, P. Gu, X. H. Zhu, Q. Yan, D. Y. Yang, *Physica B*, 545 (2018) 197.
18. M. D. Segall, P. J. D. Lindan, M. J. Probert, C. J. Pickard, P. J. Hasnip, S. J. Clarck, M. C. Payne, *J.*

Phys.: Condens. Matter, 14 (2002) 2717.
19. Q. Chen, J. Xu, S. Y. Cao, M. S. Fu, M. Wang, F. Gao, *J. Phys. Chem. Solids*, 122 (2018) 130.
20. G. Kresse, D. Joubert, *Phys. Rev. B*, 59 (1999) 1758.
21. B. Adolph, J. Furthmüller, F. Bechstedt, *Phy. Rev. B: Condens. Matter*, 63 (2001) 125108.
22. P. Käckell, B. Wenzien, F. Bechstedt, *Phys. Rev. B: Condens. Matter*, 50 (1994) 10761.
23. Y. Wang, J. P. Perdew, *Phys. Rev. B*, 44 (1991) 13298.
24. J. P. Perdew, K. Burke, M. Ernzerhof, *Phys. Rev. Lett.*, 77 (1996) 3865.
25. J. P. Perdew, Y. Wang, *Phys. Rev. B*, 45 (1992) 13244.
26. A. I. Liechtenstein, V. I. Anisimov, J. Zaanen, *Phys. Rev. B: Condens. Matter*, 52 (1995) R5467.
27. O. Bengone, M. Alouani, P. Blochl, J. Hugel, *Phys. Rev. B*, 62 (2000) 16392.
28. F. Zhou, M. Cococcioni, K. Kang, G. Ceder, *Electrochem. Commun.*, 6 (2004) 1144.
29. H. Jmonkhorst, J. D. Pack, *Phys. Rev. B*, 13 (1976) 5188.
30. Y. Y. Chen, Y. Sun, X. J. Huang, *Comp Mater Sci*, 115 (2016) 109.
31. T. F. Yi, C. Y. Li, Y. R. Zhu, J. Shu, R. S. Zhu, *J. Solid State Electrchem.*, 13 (2009) 913.
32. M. Y. Mo, K. S. Hui, X. T. Hong, J. S. Guo, C. C. Ye, A. J. Li, N. Q, Z. Z. Huang, J. H. Jiang, J. Z. Liang, H. Y. Chen, *Appl. Surf. Sci*., 209 (2014) 412.
33. J. Mao, M. G. Ma, P. P. Liu, J. H. Hu, G. S. Shao, V. Battaglia, K. H. Dai, G. Liu, *Solid State Ion*, 292 (2016) 70.
34. Y. Koyama,Y. Makimura, I. Tanaka, H. Adachi, T. Ohzuku, *J. Electrochem. Soc*., 151 (2004) A1499.